Accelerating Ocean Currents Analysis: Tiling-Based Parallel Computing for SAR Imagery

M. A. Iqbal[†], E. Kalogirou[*,†], D. Makri[*,†], C. Mettas[*,†], M. Tzouvaras[*,†], D. G. Hadjimitsis[*,†]

[†]ERATOSTHENES Centre of Excellence, Limassol 3012, Cyprus
[*]Department of Civil Engineering and Geomatics, Cyprus University of Technology, Limassol 3036, Cyprus

ABSTRACT

High-resolution synthetic aperture radar (SAR) data processing for marine applications is computationally demanding due to large memory requirements. A novel parallel approach for SAR image clustering is introduced, leveraging MATLAB's distributed computing to achieve fast and precise SAR image segmentation. We make use of this efficient parallel computing framework for Doppler centroid estimation (DCE) using the correlation Doppler estimator (CDE) and sign Doppler estimator (SDE). An onboard tiling method partitions the SAR scene into tiles of blocks, enabling localized estimation of the baseband Doppler centroid component f_{DC}. These estimates are unwrapped across range and azimuth while preserving resolution. Rigorous quality control ensures accuracy, and Doppler signatures are analyzed to derive ocean surface currents (OSC). The proposed parallelized approach reduces computational load by 32 times, enabling near-real-time OSC estimation for operational SAR-based ocean monitoring. Moreover, statistical indicators including bias, correlation, and slope are promising and validate the effectiveness of parallel computed coarse data for marine applications.

Keywords: Parallel Computing, Doppler Estimation, Ocean Currents, SAR

1. INTRODUCTION

Synthetic aperture radar (SAR) has been a key technology in Earth observation (EO) for remote sensing for over the past several decades and has played a crucial role in marinetime applications for marine safety and coastal engineering.[1] Its ability to generate high-resolution radar images through platform displacement makes it indispensable for continuous environmental monitoring. Unlike optical sensors, SAR operates independently of weather conditions and sunlight, making it highly effective for persistent maritime surveillance and oceanographic studies.[2]

One of SAR's critical capabilities is its ability to detect and analyze motion-induced Doppler shifts caused by the relative movement between the sensor and the target. The Doppler centroid frequency (f_{DC}) is a key parameter in SAR signal reconstruction, influencing image quality and the extraction of dynamic surface features.[3] Accurate estimation f_{DC} is particularly valuable in oceanographic applications, as it enables the assessment of OSC, which is crucial for marine climate, ship navigation safety, and marine ecosystem monitoring. High-resolution SAR data analysis, particularly for f_{DC} estimation, requires extensive data storage and involves slow computation, making it unsuitable for onboard applications. A lot of work has been done in this context; however, an efficient computational technique is needed for real-time estimation of ocean currents, hurricanes, and rip currents while maintaining SAR resolution.[4,5]

The parallel computing (PC) technique proposed in the past is modified as a promising solution for accelerating real-time SAR image processing and physical parameter estimation.[6] By making use of PC, the existing f_{DC} method can be optimized to significantly reduce computational time and memory usage. This approach involves partitioning high-resolution SAR data into smaller, independent tiles, each containing a subset of the dataset. These tiles are then processed concurrently across multiple computing units, effectively distributing the computational workload. As a result, memory requirements are minimized, and processing efficiency is significantly enhanced, making real-time applications more feasible for onboard systems.[7] In this paper, we propose a

For more information: (Send correspondence to M. A. Iqbal) E-mail: muhammadamjad.iqbal@eratosthenes.org.cy

Eleventh International Conference on Remote Sensing and Geoinformation of the Environment (RSCy2025), edited by Andreas Christofi, et al., Proc. of SPIE Vol. 13816 · © The Authors. Published under a Creative Commons Attribution CC-BY 4.0 License · doi: 10.1117/12.3070192

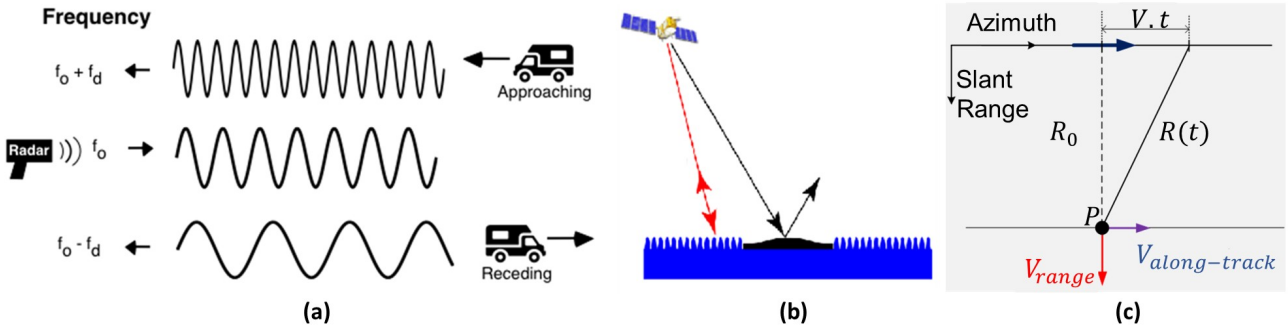

Figure 1: (a) Concept of Doppler; (b) Bragg scattering from ocean Doppler; and (c) Doppler shift produced in radar 2D signals.

modification of two state-of-the-art (SOA) f_{DC} estimation techniques by exploiting PC to achieve significantly faster processing while preserving the high-resolution integrity of SAR data. Designed technique ensures that the spatial coherence and physical signatures of f_{DC} parameters remain intact, enabling more accurate and real-time ocean circulation analysis without compromising data fidelity.

2. METHODOLOGY

Moving objects produce glare in the SAR imagery, where along-track movement causes blurring, while cross-track movement causes displacement. This displacement of an object in SAR can be translated into a Doppler shift. The concept of Doppler is given in Fig. 1(a). When a target moves, it causes a change in frequency.

2.1 Concept of Doppler Shift

Ocean waves pave a Doppler characteristic and in extreme events, these become hurricanes. As shown in Fig. 1(b), the SAR signal is reflected back from ocean bragg waves, and in case ocean waves are silent or on land, the SAR signals reflect in another direction. The Doppler effect is of minimal significance within a single pulse, but it becomes the predominant factor influencing the phase of the received signal in the azimuth direction over subsequent pulses. The relationship between the slant range and azimuth time can be mathematically represented as:

$$R(t) = \sqrt{R_0^2 + v^2 t^2} \tag{1}$$

where R_0 refers to the range at which the point target is in closest proximity to the radar and vt represents the displacement of the radar, as shown in Fig. 1(c).

2.2 Parallel Computing (PC) for SAR Data Analysis

The utilization of high-resolution SAR data for specific applications faces a significant constraint in the form of large memory system requirements. This PC solution entails dividing the SAR data images into smaller tiles that are processed independently. Each tile includes a subset of the data with a parallel computing strategy; the processing effort can be divided among multiple computing units, considerably reducing memory requirements and enhancing processing efficiency.

Given a SAR image matrix S of size $H \times W$, we define a tiling approach with tile size $T_h \times T_w$ and overlapping regions of size $O_h \times O_w$ along the height and width, respectively. The tile indices in the azimuth (height) and range (width) dimensions are defined as:

$$\begin{aligned} L_x &= \{0, O_w, 2O_w, \ldots, W - T_w\}, \\ L_y &= \{0, O_h, 2O_h, \ldots, H - T_h\}. \end{aligned} \tag{2}$$

where L_x and L_y represent the starting positions of the tiles in the range and azimuth directions, respectively. If the last tile does not completely cover the image, an additional tile is added at the end to ensure complete coverage. For each tile $I_{m,n}$ defined by its top-left coordinate (x_m, y_n) and bottom-right coordinate $(x_m + T_w, y_n + T_h)$, the Doppler centroid frequency f_{DC} is estimated using two approaches discussed below.

2.3 Correlation Doppler Estimation (CDE)

The CDE method estimates the Doppler centroid frequency, f_{DC}, by leveraging the SAR azimuth shift, correlation coefficient, and pulse repetition frequency (PRF). To achieve this, the SAR signal $S(\eta, \tau)$ is correlated with its azimuth-shifted version, forming the correlation function:

$$\begin{aligned} C(\eta,\tau) &= \sum_{\eta} S(\eta,\tau) S^{*}(\eta+\Delta\eta,\tau), \\ \phi(\eta,\tau) &= \arg\left(\sum_{k=1}^{N} C(\eta,\tau_k)\right), \\ f_{\mathrm{DC}}^{\mathrm{CDE}}(\eta,\tau) &= -\frac{\mathrm{PRF}}{2\pi}\phi(\eta,\tau). \end{aligned} \tag{3}$$

Here, ϕ represents the phase of the correlation function C, which is estimated using a sum mean kernel in the range direction. The variable k denotes the number of cross-correlation coefficients averaged to obtain the phase estimate. Finally, the Doppler centroid frequency, $f_{\mathrm{DC}}^{\mathrm{CDE}}$, is computed using the PRF and phase correlation function.[4]

2.4 Sign Doppler Estimation (SDE)

The SDE technique utilizes correlation similarly to the CDE method, but with a different calculation approach. By analyzing only the sign (via sign comparison), it becomes feasible to deduce the correlation properties of the process, leveraging its Gaussian characteristics. This estimation method exhibits reduced computational complexity and, furthermore, avoids assigning excessive weights to bright or strong reflectors, resulting in decreased sensitivity to dynamic scenes. The core principle of this method relies on the arcsine law inherent in a Gaussian process.[8] The transformed signal Y and its sign function $Z(t)$ are defined as:

$$\begin{aligned} Y &= \sin\left(\frac{\pi}{2} R\left[II, IQ, QI, QQ\right]\right), \\ Z(t) &= \begin{cases} 1, & \text{for } Y(t) \geq 0, \\ -1, & \text{for } Y(t) < 0. \end{cases} \end{aligned} \tag{4}$$

Since $Z(t)$ only takes values of $+1$ and -1, it represents the sign of $Y(t)$. To estimate the Doppler, the first step is to compute four sign correlations, including II, IQ, QI, and QQ. The corresponding correlation coefficients and complex correlation coefficients are then obtained as:

$$\begin{aligned} R(k) &= \frac{1}{2}(\rho_{II} + \rho_{QQ}) + j\frac{1}{2}(\rho_{IQ} - \rho_{QI}), \\ f_{\mathrm{DC}}^{\mathrm{SDE}} &= \frac{\mathrm{PRF}}{2\pi\Delta\delta} \times \arg\{R(k)\}. \end{aligned} \tag{5}$$

It is important to highlight that the calculation of Y essentially involves counting how often two azimuth-shifted samples have the same sign.

2.5 Ocean surface current (OSC) estimation

The radar imaging model (RIM) aids in estimating OSC, including eddies, breaking waves, and rip currents. To extract the OSC from SAR data, the RIM model is adapted using the line-of-sight component and f_{DC}, given as:

$$U_{\mathrm{D}} = -\frac{\pi f_{\mathrm{DC}}}{k_r \sin\theta}, \text{ whereas, } k_r = \frac{2\pi}{\lambda} = \frac{2\pi f_{\mathrm{rad}}}{c} \tag{6}$$

The parameter θ denotes the incident angle, and the wave number k_r is derived from the radar frequency, where λ and f_{rad} correspond to the sensor wavelength and radar frequency, respectively. The speed of light is given by c, and for Sentinel-1, the calculated value of k_r is 113.28 m^{-1}.[9]

2.6 Comparison and Assessment

Given the equations in (7–9), which represent key statistical measures for assessing the relationship between two variables for comparison:

- **Bias**:
  Bias calculates the average difference between predicted ($\hat{y}_i$) and actual (y_i) values, indicating systematic error.

$$\text{Bias} = \frac{1}{n}\sum_{i=1}^{n}(\hat{y}_i - y_i) \tag{7}$$

- **Correlation Coefficient** (r):
  The correlation coefficient quantifies the strength and direction of the linear relationship between two methods, ranging from 0 to 1.

$$r = \frac{\sum(x_i - \bar{x})(y_i - \bar{y})}{\sqrt{\sum(x_i - \bar{x})^2}\sqrt{\sum(y_i - \bar{y})^2}} \tag{8}$$

- **Slope** (m):
  Slope in linear regression represents the rate of change in y with respect to x, showing how much y changes per unit increase in x.

$$m = \frac{\sum(x_i - \bar{x})(y_i - \bar{y})}{\sum(x_i - \bar{x})^2} \tag{9}$$

These metrics are important in regression analysis, error evaluation, and method performance assessment.

3. EXPERIMENTAL RESULTS

SAR scans wide areas in hundreds of kilometers and keeps data for on-board physical parameter estimation. Memory for data is a constraint and computation of Doppler and OSC from SAR scenes takes a long time. The goal of this parallel computing is to gain understanding of the most efficient utilization of existing computing resources in order to reduce the duration of processing during the events of marine emergencies.

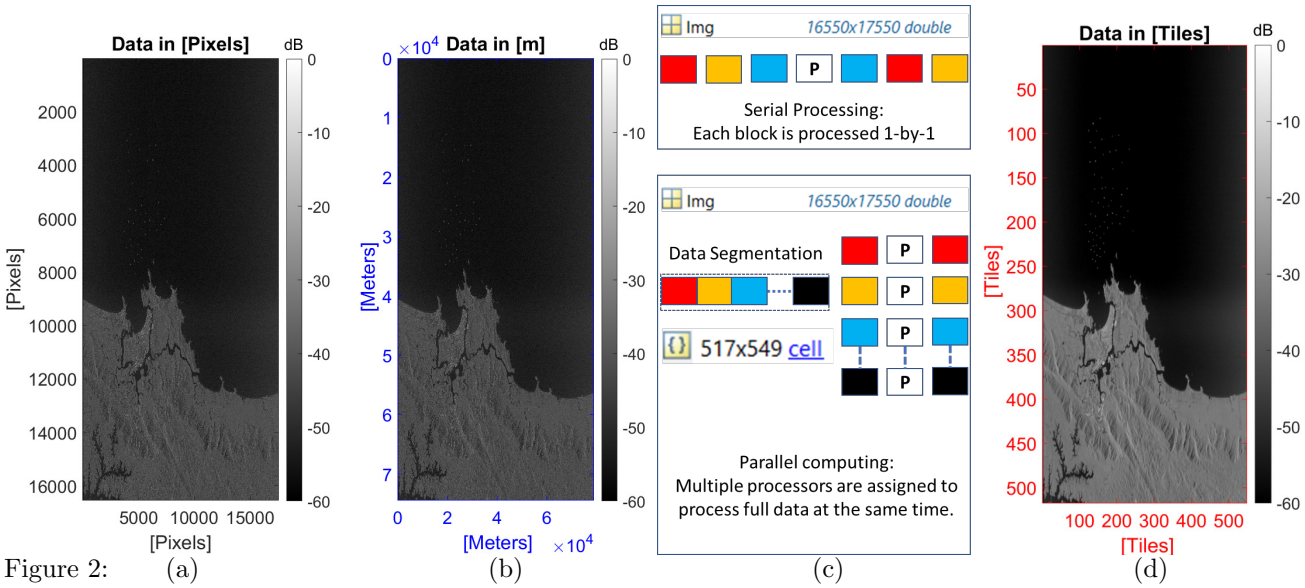

Figure 2: (a) (b) (c) (d)
(a) SAR scene represented in pixels, (b) SAR scene represented in meters, (c) concept of serial and parallel computing, and (d) SAR scene after applying parallel computing.

The Sentinel-1 intensity image of a single-look complex (SLC) SAR scene is presented in Fig. 2(a), with an initial resolution of azimuth × range = 16,650 × 17,750 pixels. By applying the pixel spacing provided in the SAR data product metadata for both azimuth and range directions, the corresponding ground coverage is computed as azimuth × range = 74.925 × 79.875 km, as shown in Fig. 2(b). This results in a substantial demand for memory resources.

To mitigate computational and memory constraints while preserving the spatial integrity of the desired output, a tiling strategy is employed, as illustrated in Fig. 2(c). This approach enables parallel processing at an appropriate scale, significantly reducing computational costs. The processed SAR scene, depicted in Fig. 2(d), demonstrates that the estimated features remain well preserved, with sufficient resolution for accurately distinguishing the SAR scene signatures. The dataset is partitioned into azimuth × range = 549 × 517 tiles, leading to an approximate 32-fold reduction in computational time.

Parallel computing has been directly implemented for SAR data processing and optimized using two Doppler estimation methods: the CDE and the SDE. The estimated f_{DC} signature from CDE and its corresponding OSC are illustrated in Fig. 3(a) and Fig. 3(b), respectively. Similarly, the f_{DC} signature extracted from SDE and its associated OSC are shown in Fig. 3(c) and Fig. 3(d). Due to differences in methodology, slight variations in the extracted signatures can be observed, particularly near the shoreline, where high-speed waves interact with the coastline. However, the qualitative results remain within acceptable error bounds, making them suitable for observation and monitoring applications.

Fig. 4(a) and (b) present the spatial signatures of ocean surface currents, overlaid with the magnitude and direction of the current fields estimated using Doppler information from the CDE and SDE methods, respectively. While these techniques differ methodologically, they yield similar spatial patterns for the OSC field, with only minor variations in magnitude.

The original SAR dataset occupies 1024 MB of memory, whereas the parallel-computed version requires only 32 MB. Additionally, the Doppler and OSC signatures derived from pixel data have been reduced from 776 MB to 24.25 MB each. The computational time has significantly decreased from 192 s to just 6 s. This efficiency improvement highlights the potential of parallel computing for real-time marine surveillance, particularly during nighttime, low-visibility conditions, or in scenarios where hurricanes are distant from the coastline. Moreover, the proposed approach facilitates time-series monitoring while optimizing resource utilization, memory consumption, and computational efficiency.

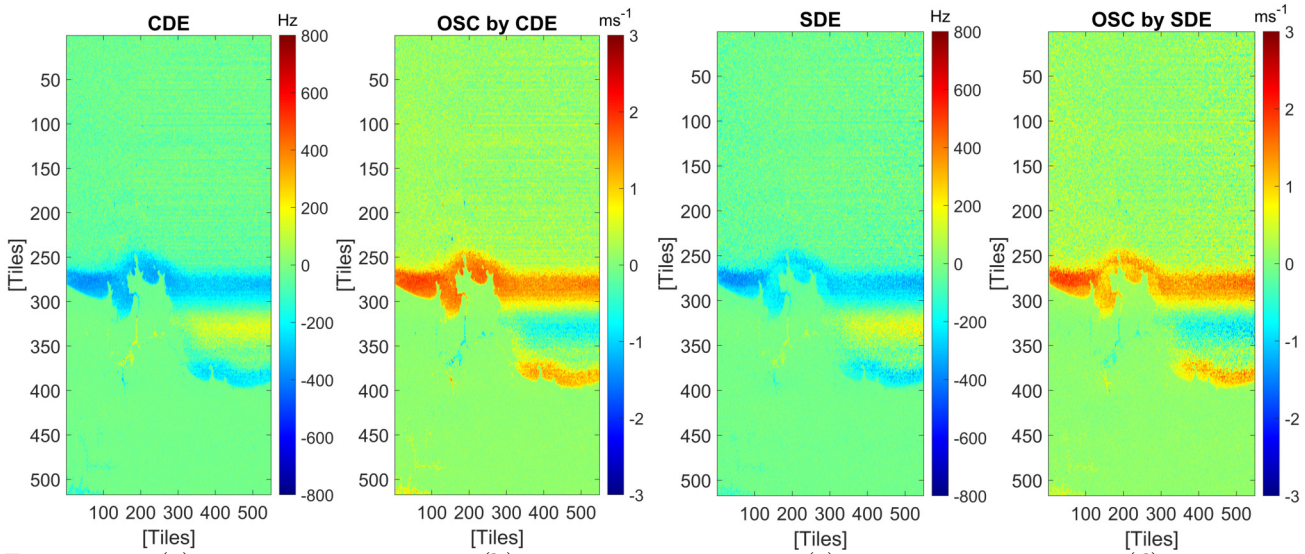

Figure 3: (a) Signature of f_{DC} estimated using CDE, and (b) its retrieved OSC. (c) Signature of f_{DC} estimated using SDE, and (d) its extracted OSC.

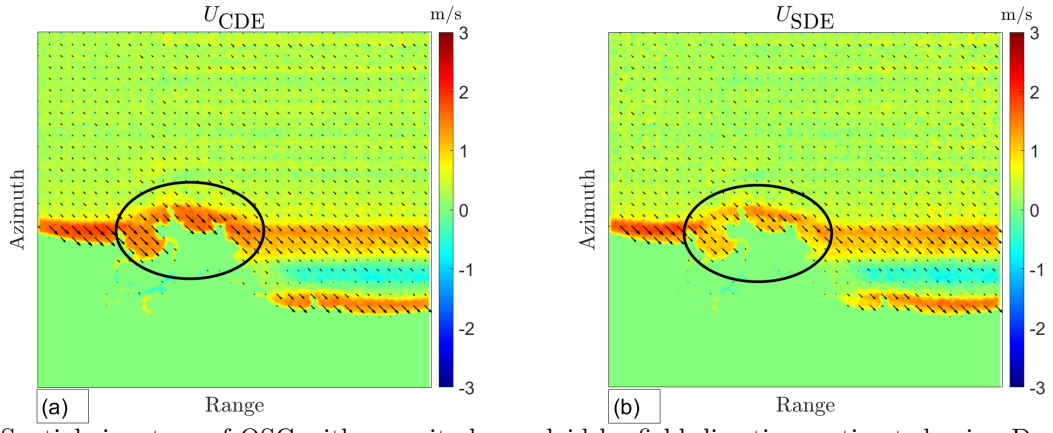

Figure 4: Spatial signature of OSC with magnitude overlaid by field directions estimated using Doppler information from (a) CDE and (b) SDE, respectively.

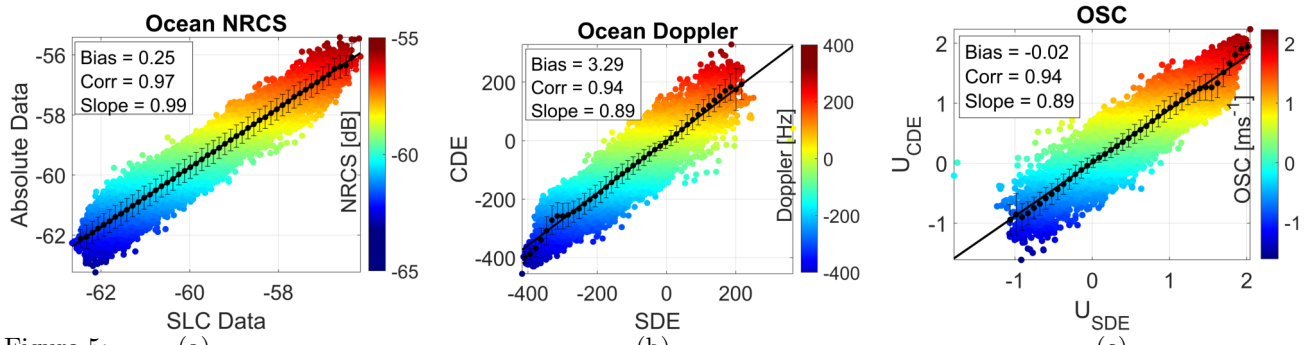

Figure 5: Comparison over the ocean for SLC SAR data and absolute SAR data; (a) NRCS; (b) f_{DC}; and (c) OSC.

Table 1: Quantitative and computational analysis of given parameters derived from two data types or methods.

Parameter	Bias	Correlation (r)	Slope	Memory (pixel)	Memory (Tile)	$T_{\mathbf{Proc}}$
NRCS	0.25	0.97	0.99	1024 MB	32 MB	192 s
Doppler	3.29	0.94	0.89	776 MB	24.25 MB	6 s
OSC	-0.02	0.94	0.89	776 MB	24.25 MB	6 s

Quantitative analysis of physical parameters is done among two types of data (for NRCS) and two methods (for Doppler and OSC). The scatter plots of NRCS, Doppler centroid, and OSC over the ocean region of interest (ROI) are given in Fig. 5(a), 5(b), and 5(c), respectively. The color bars indicate the value of those physical parameters over ocean ROI. Statistical comparisons are highlighted in the text box for each case. Moreover, computational analyses are disclosed in Table 1. We have examined that the memory requirement as well as processing time T_{Proc} for data is reduced by 32 times, with minimal resolution loss. This ground-breaking, efficient computational solution brings us very close to adapting it for real-time ocean currents analysis, particularly during hurricanes and floods in coastal areas.

Physical Limitations: Compared to the Energy Balancing (EB) method,[10] which tends to be dominated by non-homogeneous SAR scenes, the methods (CDE and SDE) are implemented in such challenging environments and show comparable performance. Spatial signature analysis and quantitative evaluation indicate that these two methods are strong candidates for OSC retrieval under a variety of SAR scene conditions. In contrast, the EB method, due to its reliance on spectral balancing, often detects Doppler signatures over land when tracking moving objects. Moreover, the CDE and SDE methods are not sensitive to, nor limited by, physical constraints or adverse marine conditions, including high wind gusts, low wind speeds, or dark SAR images.

4. DISCUSSION AND CONCLUSION

SAR is a powerful active remote sensing technology with key applications in marine hazards safety. However, processing wide-swath SAR data poses significant challenges due to high memory storage requirements and extensive computational time. To address these limitations, proposed parallel computing enables efficient data processing by dividing SAR data into tiles, allowing independent processing across multiple computing units based on tile size. This approach significantly reduces memory consumption and computational load while preserving SAR's spatial resolution and the physical integrity of OSC signatures. Consequently, the proposed computational framework enhances the accuracy and efficiency of real-time ocean circulation analysis without compromising data fidelity.

ACKNOWLEDGMENTS

The 'EXCELSIOR' project has received funding from the European Union's Horizon 2020 research and innovation program under Grant Agreement No. 857510, from the Government of the Republic of Cyprus through the Directorate General for the European Programmes, Coordination and Development, and the Cyprus University of Technology. The authors also acknowledge the 'EXCELSIOR': ERATOSTHENES: Excellence Research Centre for Earth Surveillance and Space-Based Monitoring of the Environment H2020 Widespread Teaming project (www.excelsior2020.eu), in which the Eratosthenes CoE has been established.

REFERENCES

[1] Asiyabi, R. M., Ghorbanian, A., Tameh, S. N., Amani, M., Jin, S., and Mohammadzadeh, A., "Synthetic aperture radar (SAR) for ocean: A review," *IEEE Journal of Selected Topics in Applied Earth Observations and Remote Sensing* **16**, 9106–9138 (2023).

[2] Tomiyasu, K., "Tutorial review of synthetic-aperture radar (SAR) with applications to imaging of the ocean surface," *Proceedings of the IEEE* **66**(5), 563–583 (1978).

[3] Won, J.-S., "Doppler frequency estimation of point targets in the single-channel SAR image by linear least squares," *Remote Sensing* **10**(7), 1160 (2018).

[4] Iqbal, M. A., Anghel, A., and Datcu, M., "Doppler centroid estimation for ocean surface current retrieval from sentinel-1 SAR data," in [*2021 18th European Radar Conference (EuRAD)*], 429–432 (2022).

[5] Fan, S., Zhang, B., Moiseev, A., Kudryavtsev, V., Johannessen, J. A., and Chapron, B., "On the use of dual co-polarized radar data to derive a sea surface doppler model—part 2: Simulation and validation," *IEEE Transactions on Geoscience and Remote Sensing* **61**, 1–9 (2023).

[6] Bhattacharya, C., "Parallel processing of satellite-borne SAR data for accurate and efficient image formation," in [*8th European Conference on Synthetic Aperture Radar*], 1–4 (2010).

[7] Gou, S., Zhuang, X., Zhu, H., and Yu, T., "Parallel sparse spectral clustering for SAR image segmentation," *IEEE Journal of Selected Topics in Applied Earth Observations and Remote Sensing* **6**(4), 1949–1963 (2013).

[8] Madsen, S., "Estimating the doppler centroid of SAR data," *IEEE Transactions on Aerospace and Electronic Systems* **25**(2), 134–140 (1989).

[9] Iqbal, M. A., Mohammadi Asiyabi, R., Ghozatlou, O., Anghel, A., and Datcu, M., "Towards complex-valued deep architectures with data model preservation for sea surface current estimation from SAR data," in [*Proceedings of the 20th International Conference on Content-based Multimedia Indexing*], 146–152 (2023).

[10] Yang, J., Liu, C., and Wang, Y., "Adaptive doppler centroid estimation algorithm of airborne SAR," *IEICE Electronics Express* **9**(13), 1135–1140 (2012).